ISBN: 978-3-95450-179-3 doi:10.18429/JACoW-FEL2017-MOP018

DISTRIBUTED SELF-SEEDING SCHEME FOR LCLS-II*

Chuan Yang[1,2†], Juhao Wu[1‡], Guanqun Zhou[1,3], Bo Yang[4],
Cheng-Ying Tsai[1], Moohyun Yoon[1,5], Yiping Feng[1], Tor Raubenheimer[1]
[1]SLAC National Accelerator Laboratory, Menlo Park, California, USA
[2]NSRL, University of Science and Technology of China, Hefei, Anhui, China
[3]Institute of High Energy Physics, and UCAS, Chinese Academy of Sciences, Beijing, China
[4]University of Texas at Arlington, Arlington, Texas, USA
[5]Department of Physics, Pohang University of Science and Technology, Pohang, Korea

Abstract

Self-seeding is a successful approach for generating high-brightness X-ray free electron laser (XFEL). A single-crystal monochromator in-between the undulator sections to generate a coherent seed is adopted in LCLS. However, for a high-repetition rate machine like LCLS-II, the crystal monochromator in current setup cannot sustain the high average power; hence a distributed self-seeding scheme utilizing multi-stages is necessary. Based on the criteria set on the crystal, the maximum allowed X-ray energy deposited in the crystal will determine the machine configuration for such a distributed self-seeding scheme. In this paper, a distributed self-seeding configuration is discussed for LCLS-II type projects in the hard X-ray FEL energy regime. The study is carried out based on numerical simulation.

INTRODUCTION

Linac Coherent Light Source (LCLS), the world's first hard X-ray FEL has been successfully operated in SASE mode [1]. Conventional SASE FEL has full transverse coherence, but the longitudinal coherence is limited [1,2]. In order to improve the longitudinal coherence, self-seeding scheme has been proposed [3]. A self-seeding X-ray FEL consists of two undulator sections separated in a drift section by a monochromator and an electron by-pass chicane. A grating monochromator was adopted for the soft X-ray [3], while a single crystal monochromator oriented in Bragg transmission geometry can be used for the hard X-ray [4]. The radiation generated by the first undulator section and the electron beam are separated in the drift section between the two undulator sections. The radiation passes through the monochromator, which can filter the radiation spectrum. The electron beam passes through the chicane, which washes out the micro-bunching induced by the first undulator section and delays the electron beam relative to the radiation pulse. The purified radiation and the electron beam are recombined at the entrance of the second undulator section, through which the radiation is amplified up to saturation.

The operation of self-seeding has been successfully achieved at LCLS, in which the repetition rate is 120 Hz. However, LCLS-II FEL project is designed to operate at a higher repetition rates of 0.93MHz. In this case, the heat load on the monochromator will become an issue and limit the maximal seed power. The multi-stages self-seeding scheme can generate higher spectral purity, which can reduce the heat load of the monochromator.

For the LCLS-II hard X-ray self-seeding (HXRSS) baseline undulator system, there will be two 'missing segments' after segment 7 and 14, which are reserved for self-seeding station shown in Fig. 1. This two-stages self-seeding configuration was considered for the photon energy range of (4 keV~8 keV). In this paper, we study the two-stage self-seeding configuration for LCLS-II project with GENESIS simulation code [5] for 4 keV and 8.3 keV hard X-ray with LCLS-II parameters. All the data refer to single shot realization.

Table 1: The Relevant Parameters used in 4keV and 8.3keV Simulation.

Parameters	Value	Unit
Electron beam energy	4.0/8.0	GeV
Energy spread	0.5	MeV
Peak current	1/3	kA
Normalized emittance	0.45	mm-mrad
FEL photon energy	4/8.3	keV
Charge	100/300	pC
Undulator parameter K	0.96/1.91	-
Undulator period	2.6	cm
Number of period per undulator section	130	-
Total number of sections	32	-
Drift length	1.17	m

NUMERICAL SIMULATION

4-keV Self-Seeding Simulation

Here we focus on 4keV self-seeding simulation to study LCLS-II HXRSS project in the low photon energy range. The baseline undulator system is shown in Fig. 1. Relevant simulation parameters are presented in Table 1. We assume that the average betatron function is 17.0 m. In the two monochromators, we choose symmetric diamond C(111) crystal to generate the wake seed, and the crystal thickness is 30 μm. The two crystal monochroma-

* The work was supported by the US Department of Energy (DOE) under contract DE-AC02-76SF00515 and the US DOE Office of Science Early Career Research Program grant FWP-2013-SLAC-100164.
† chuany@SLAC.Stanford.EDU
‡ jhwu@SLAC.Stanford.EDU

ISBN: 978-3-95450-179-3 doi:10.18429/JACoW-FEL2017-MOP018

tors act as bandstop filters for the radiation pulse. The modulus and the phase of the crystal transmissivity shown in Fig. 2 are calculated with the help of xop.2.4 [6] and Kramers–Kronig relations [7,8].

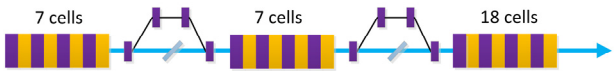

Figure 1: Design of LCLS-II hard X-ray baseline undulator system including two 'miss undulators' which are reserved for self-seeding operation.

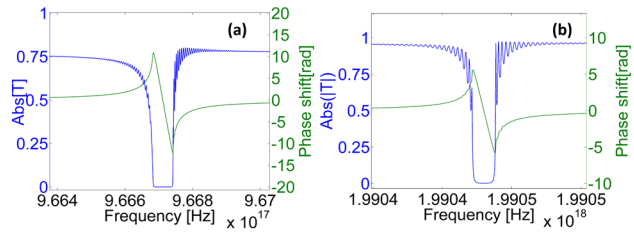

Figure 2: (a) Modulus and phase of transmissivity for symmetric C(111) Bragg reflection from perfect diamond crystal at 4keV. (b) Modulus and phase of transmissivity for symmetric C(400) Bragg reflection from perfect diamond crystal at 8.3 keV.

The spectrum and power at the end of the 7th undulator section are shown in Fig. 3 (a) and (b). Figures 3 (c) and (d) show the spectrum and the wake seed after the first crystal. The bunch, with flat top length about 28 µm, overlap with the wake seed in the red window as in the Fig. 3 (d).

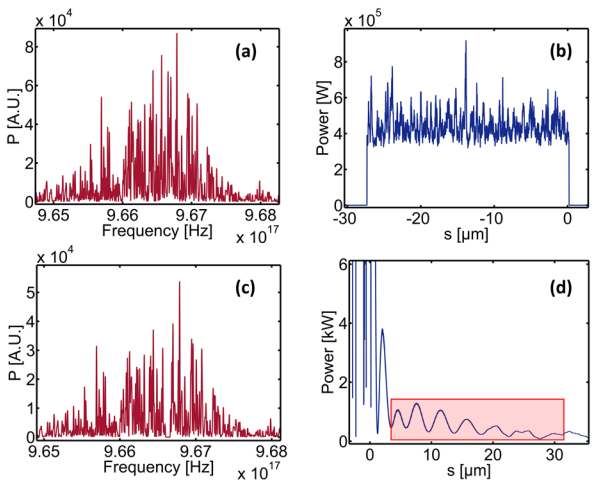

Figure 3: (a) The spectrum before the first crystal. (b)The power before the first crystal. (c) The spectrum after the first crystal. (d)The power after the first crystal. The red window is the overlap region for the electron beam and the wake seed.

The seed is amplified in the second undulator section and then impinges on the second crystal monochromator. The spectrum and power before the second crystal shown in Fig. 5. The spectrum and power after the second crystal is shown in Fig. 6.

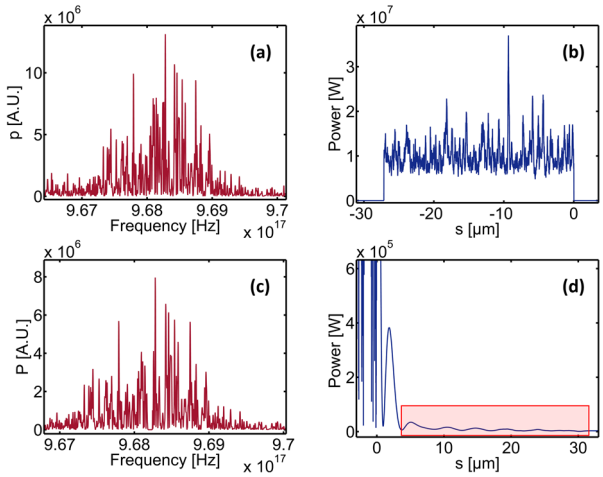

Figure 4: (a) The spectrum before the second crystal. (b)The power before the second crystal. (c) The spectrum after the second crystal. (d)The power after the second crystal. The red window is the overlap region for the electron beam and the wake seed.

After the second crystal, the seed is amplified to saturation in the final undulator section. The output spectrum and power are shown in Figure 5. The energy per pulse imping on the second crystal is about 0.8 µJ, and the transverse rms of the electron bunch is 50 µm. The angle between the X-ray and the crystal surface is 48.8°. Therefore, the average power density is close to 80 W/mm².

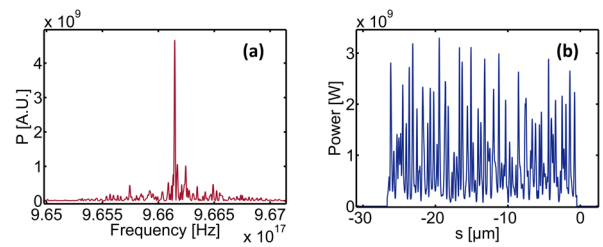

Figure 5: The spectrum (a) and power (b) at the end of the final undulator section.

According to the simulation, the seed power after the first crystal is about 1.2 kW shown in Fig. 3 (d), which is not enough to dominate over the shot noise power. In other worlds, the location of the first crystal may not be suitable for the 4keV case. Therefore we move the first crystal to the later locations to the end of the 13th undulator section Fig. 6. The average power density on the crystal is about 100 W/mm² per second [9]. This number is one order of magnitude smaller than the average power density at the first monochromator of third generation synchrotron radiation sources.

For the crystal at the new location, the spectrum and power before the crystal are shown in Fig. 7 (a), (b). The spectrum and wake seed after the crystal are shown in

ISBN: 978-3-95450-179-3 doi:10.18429/JACoW-FEL2017-MOP018

Fig. 7 (c), (d). The seed power is about 170 kW, now enough to dominate over the shot noise power. At the end of the final undulator section, we get a purify pulse with $\Delta\omega/\omega_0 = 7\times10^{-5}$ bandwidth shown in Fig. 8 (a), which has a comparable bandwidth with the two stage case.

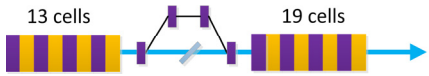

Figure 6: The assumed configuration of LCLS-II HXSS in the low photon energy range.

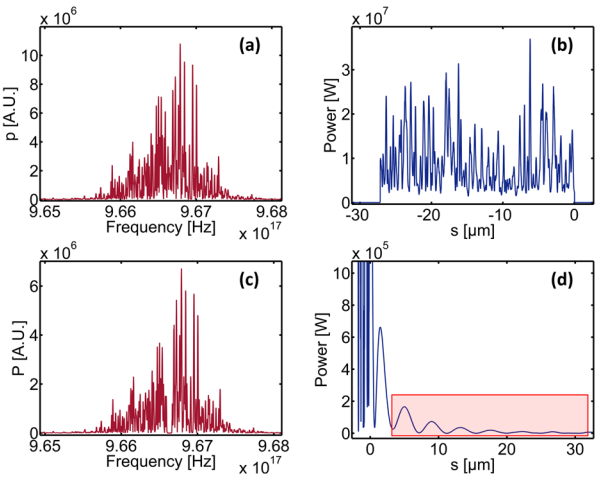

Figure 7: (a) The spectrum before the crystal. (b)The power before the crystal. (c) The spectrum after the crystal. (d)The power after the crystal. The red window is the overlap between the electron beam and the wake seed.

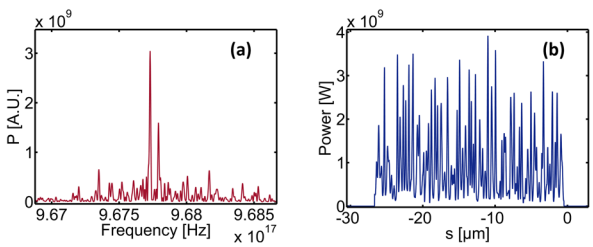

Figure 8: The spectrum (a) and power (b) at the end of the final undulator section.

8.3-keV Self-Seeding Simulation

For the high repetition rate (0.93 MHz) LCLS-II-HE high energy range, we focus on 8.3keV self-seeding simulation. The optimization of electron beam line is still on going. The assumed simulation parameters here are shown in Table 1. We assume that the average betatron function is 20.0 m. The symmetric diamond C(400) crystal is chosen to generate the wake seed, and the crystal thickness is 50 μm. The modulus and the phase of the crystal transmissivity are shown in Fig. 2 (b). The spectrum and power distribution at the end of final undulator section are shown in Fig. 9 (a), (b). The energy per pulse impinging on the second crystal is about 50 μJ, and the transverse rms of the electron bunch is 25 μm. The angle between the X-ray and the crystal surface is 56.89°. According to the simulation result, the average power density at the second crystal is close to 11 kW/mm^2 (Fig. 10), two orders of magnitudes higher than the average power density on the crystal at third generation synchrotron radiation. This power density has exceeded the threshold. One way to resolve this heat load issue is to decrease the repetition rate to tens of kHz.

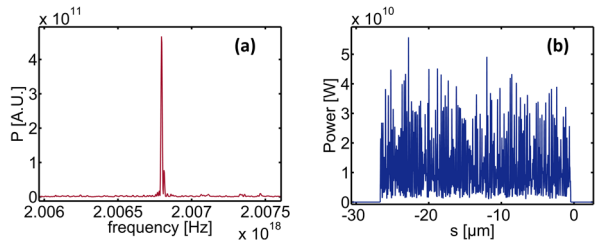

Figure 9: The spectrum (a) and power (b) at the end of the final undulator section.

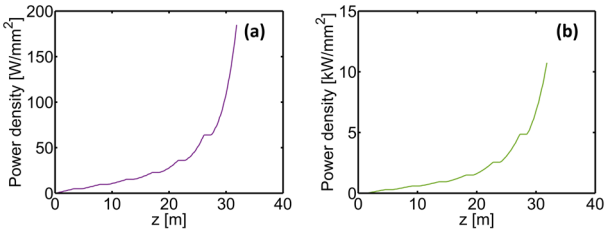

Figure 10: (a) Power density along z in the first undulator section. (b) Power density along z in the second undulator section.

SUMMARY

For the high repetition rate FEL like LCLS-II, heat load will determine the location of monochromator. For different photon energy range and different repetition machine, the optimal undulator system configuration is different. In the low energy range of LCLS-II HXRSS, from the preliminary numerical simulation above, the designed baseline of undulator system is not optimal. That is, the first monochromator after 7th undulator section is placed too early, where the seed power after the monochromator is not enough to dominate over the shot noise power within the gain bandwidth. Therefore, the location of the crystal may be after the 13th undulator section. In this new configuration, one stage self-seeding is sufficient to generate a purity spectrum. In the high-energy range of LCLS-II HXRSS, if based on the baseline design and the assumed simulation parameters in Table 1, the allowed operating repetition rate of self-seeding is in tens of kHz. We have present a preliminary simulation in this paper, more dedicated simulation work is in progress.

ISBN: 978-3-95450-179-3 doi:10.18429/JACoW-FEL2017-MOP018

REFERENCES

[1] Emma, P. *et al*., "First lasing and operation of an angstrom-wavelength free-electron laser" *Nat. Photon.,* **4**, p. 641-647 (2010).

[2] Altarelli, M. *et al*., The European X-ray Free -Electron Laser, Technical Design Report, DESY 2006 -097, Hamburg (2006).

[3] Feldhaus J. *et al*., "Possible application of X-ray optical elements for reducing the spectral bandwidth of an X-ray SASE FEL*", Optics. Comm*., **140**, 341 (1997).

[4] Gianluca G., Vitali K., and Evgeni S., "A novel self-seeding scheme for hard X-ray FELs", *J. Mod. Opt*., **58**, 1391(2011).

[5] Reiche, S., *Nucl. Instrum. Methods Phys. Res*., Sect. A **429**, 243–248 (1999).

[6] ESRF. X-ray Oriented Programs Software Package. *https://www1.aps.anl.gov/Science/Scientific-Software/XOP*

[7] Kramers, H.A.,La diffusion de la lumiere par les atomes. *Attidel Congresso Internazionale dei Fisici*; Zanichelli: Bologna, **2**, 545–557 (1927).

[8] Kronig, R.; de, L., "On the Theory of Dispersion of X-Rays" *J. Opt. Soc. Am*. **12**, 547–557 (1926).

[9] Gianluca G., *et al*., "Production of transform-limited X-ray pulses through self-seeding at the European X-ray FEL", DESY 11-165, September 2011.